

Pd Size Effect on the Gas Sensing Properties of Pd-Loaded SnO₂ in Humid Atmosphere

Nan Ma,[†] Koichi Suematsu,[‡] Masayoshi Yuasa,[§] and Kengo Shimanoe^{*,§}

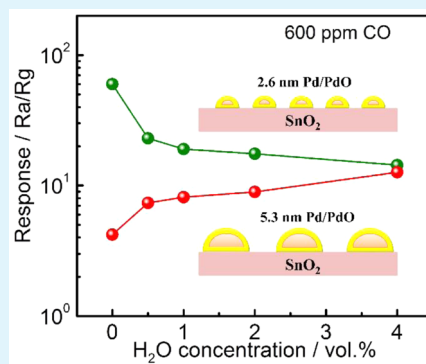
[†]Interdisciplinary Graduate School of Engineering Sciences, Kyushu University, Fukuoka 816-8580, Japan

[‡]Chemical & Textile Research Institute, Fukuoka Industrial Technology Center, Fukuoka 818-8540, Japan

[§]Faculty of Engineering Sciences, Kyushu University, Fukuoka 816-8580, Japan

ABSTRACT: Pd particles of different nanosizes were loaded on the SnO₂ surface by using different Pd precursors for the purpose of investigating the Pd size effect on gas sensing properties in humid atmosphere. One kind of Pd-loaded SnO₂ nanoparticle was characterized by smaller Pd particles (2.6 nm) with high dispersion, while another kind was characterized by larger Pd particles (5–10 nm) with low dispersion. It was found that both kinds of Pd on the SnO₂ surface let the mainly adsorbed oxygen species change from O⁻ to O²⁻ in humid atmosphere at 350 °C. In addition, the water vapor poisoning effect on electric resistance and sensor response was greatly reduced by loading Pd. Interestingly, for the CO response at 350 °C, Pd-SnO₂ with small Pd size showed almost constant sensor response with varying humidity (0.5–4 vol % H₂O). While the CO response of Pd-SnO₂ with large Pd size even increased with increasing amount of water vapor. Moreover, the former CO response was increased from 300 to 350 °C, but the later response decreased with increase in operating temperature. These behaviors were analyzed by temperature programmed reduction (TPR) in H₂ and CO atmospheres, and they were supported by the different catalytic activities of different nanosized Pd particles.

KEYWORDS: SnO₂ nanoparticles, Pd particle size, water vapor, oxygen adsorption, H₂, CO



INTRODUCTION

Tin dioxide based gas sensors are widely used in industry and daily life, due to low cost, long-term stability, and especially high sensitivity to H₂ and CO. The gas sensing mechanism is related to the change in electric resistance caused by the surface reaction between adsorbed oxygen species and target gas. Gas sensors are usually used in common environments with varying humidity. It is well-known that the existing water vapor adsorbs on the SnO₂ surface, which decreases the electric resistance of the gas sensor in a similar way to reducing gas, resulting in an interfering effect for the gas detection.^{1,2} Thus, water vapor is one of the important considerations in sensor research. However, the interaction of H₂ and CO with the SnO₂ surface in the presence of water vapor is still under discussion. Some researchers consider OH⁻ groups competing with oxygen for the same adsorption site on the SnO₂ surface.^{3,4} It was also proposed that the mainly adsorbed oxygen species on the SnO₂ surface was changed from O²⁻ in dry atmosphere to O⁻ in humid atmosphere. The sensor response is reduced in humid atmosphere due to the oxygen species change.²

It is well-known that the sensing properties of the SnO₂ gas sensor can be improved by sensitization with Pd even in humid atmosphere.¹ Electronic and chemical sensitizations are mainly proposed toward the role of Pd in the gas sensing process. The former one considers the enhanced sensor response due to the oxidation state change of Pd, which shows that a P–N junction is formed at the interface of PdO and SnO₂ in air and disappears in the reducing gas. The latter one is focused on the ability of Pd to

activate the target gas and to facilitate its catalytic oxidation on the SnO₂ surface.⁵ However, the sensitization effect of Pd was greatly influenced by the distribution state that depended a lot on the noble metal precursor, material preparation procedure, and deposition method.^{6–11} Two methods are commonly used to introduce Pd on SnO₂ nanoparticles: (1) Pd is impregnated on calcined SnO₂ and then the mixture is heat treated again; (2) Pd is introduced in the preparation process of the SnO₂ particle, followed by heat treatment. In the former case, Pd disperses on the surface of SnO₂ and the particle size of Pd-SnO₂ is independent of Pd loading. In the latter case, Pd may diffuse into the SnO₂ lattice and modify the particle size of SnO₂.^{7–9} This point has important consequences on the gas sensitivity, since the surface concentration of Pd depends on the SnO₂ surface area, which combines with the particle size of SnO₂ to affect the sensitivity.

The gas sensing mechanism is more complicated for Pd-loaded SnO₂ in humid atmosphere. It was reported that Pd may create new adsorption sites, increase the reactant for the CO sensing reaction, and decrease the activation energy of CO to make it more favorable than the adsorption of water.⁴ Additionally OH⁻ can react with CO for the Pd-loaded SnO₂ sensor, contributing to the increase of the sensor signal.¹² The

Received: May 20, 2015

Accepted: June 26, 2015

Published: June 26, 2015

catalytic doping also can activate the surrounding lattice oxygen and change the reaction route in humid atmosphere, which was reported in the Pt doped SnO₂ sensor.³ Pd on the SnO₂ surface and Pd in the bulk of SnO₂ showed a completely different CO sensing mechanism in humid atmosphere.⁴ Moreover, the distribution state of Pd also influences the gas sensing properties. It was recognized that the high dispersion of small Pd particles gives a high sensor response.^{6,7} These results suggest the importance of the Pd distribution state for improving the sensor properties.

In this paper, two kinds of Pd-loaded SnO₂ nanoparticles with different Pd sizes were prepared by introducing different Pd precursors on calcined SnO₂. A direct comparison is made possible and enables us to study the impact of Pd size and its distribution state on the gas sensing properties in the presence of water vapor. Therefore, the gas sensing performance of two kinds of Pd-loaded SnO₂ in humid atmosphere was investigated at 300 and 350 °C and the influence of Pd size and its distribution state on the gas sensing properties was further clarified.

EXPERIMENTAL SECTION

Material Preparation. The preparation process of SnO₂ nanoparticles can be described as follow: stannic acid gel was obtained by dropping SnCl₄·5H₂O solution (1M) into NH₄HCO₃ solution (1M). After centrifuging and washing by NH₄NO₃ solution (1M) 6 times, it was hydrothermally treated in an ammonia solution (pH = 10.5) under the pressure of 10 MPa at 200 °C for 3 h. Then the obtained SnO₂ sol was dried at 120 °C and heat-treated at 600 °C in oxygen atmosphere. Pd nanosized particles were loaded on SnO₂ surface by impregnation method using Pd(NH₃)₂(NO₂)₂ and Pd(NO₃)₂ aqueous solution (abbreviated them to PdNN-SnO₂ and PdN-SnO₂, respectively). The former one followed by ammonia solution treatment (pH = 9.5) and filtration process. Finally the obtained two kinds of Pd-loaded SnO₂ powders were dried at 120 °C and heat-treated at 500 °C for 3 h in air. The material preparation process was shown in Figure 1.

Material Characterization. The crystal structure of powders was analyzed by X-ray diffraction with copper K α radiation ($\lambda = 1.5418 \text{ \AA}$) filtered through a Ni foil (XRD, RINT 2100, Rigaku, Japan). The crystallite size of powder was calculated from the (110) peak of XRD pattern by Scherrer equation. Specific surface area was measured by surface area analyzer (BET, BELSOR, BEL, Japan). The microstructure was observed by transmission electron microscopy (TEM) (Tecnai-F20, FEI, US). The obtained Pd loading amount on SnO₂ surface was determined by energy dispersive X-ray fluorescence spectrometer (XRF, EDX-800, Shimadzu, Japan).

CO pulse adsorption method (BEL-CAT, BEL, Japan) was used to detect the particle size, dispersion and surface area of Pd, which is one of the most effective methods to check the distribution state of catalyst on supporting material.^{13–15} For CO pulse adsorption, it was found that no CO adsorbed on the surface of neat SnO₂. Temperature-programmed reduction by hydrogen (H₂-TPR) and CO (CO-TPR) was carried out in a flow of 1000 ppm of H₂/N₂ and CO/N₂, respectively (BEL-CAT, BEL, Japan). The pretreatment and measurement process for CO pulse adsorption and TPR were same as previously report.¹⁶

Sensor Fabrication and Electric Measurement. The obtained powders were mixed with appropriate amount of α -terpineol to form uniform paste, and then screen-printed on an alumina substrate (9 × 13 × 0.38 mm³) with Au electrodes (line width: 180 μm , distance between lines: 90 μm , sensing area: 64 mm²). The resulting devices (thickness: 30–40 μm) were heat-treated at 580 °C for 3 h in air to remove the organic binder and stabilize the sensing layer. The measurements were carried out in a conventional gas flow apparatus equipped with gas pretreatment system, water vapor introduction system, sensor measurement chamber, humidity sensor and oxygen sensor (zirconia oxygen cell). The gas pretreatment system was consisted of Pt/Al₂O₃ catalyst (5 wt %, Wako Pure Chemical Industries, Ltd.) and molecularsieves (5A 1/16, Wako Pure Chemical Industries Ltd.) to remove impurity gases

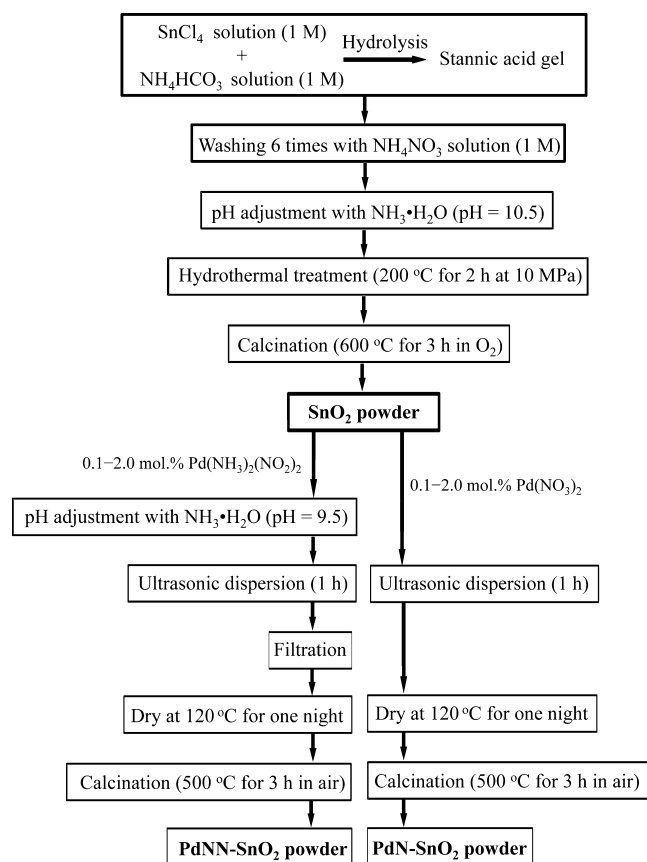


Figure 1. Flowchart for the preparation of Pd-loaded SnO₂ powder.

(such as CO and hydrocarbon) and water, respectively. Before measurement, sensors were pretreated at 580 °C for 2 h in humidity of 4 vol % H₂O and then reduced to 300 or 350 °C with keeping the same humidity.¹⁶ After the electric resistance kept stable, the humidity changed to the designated amount. The electric resistance was measured under the flow of 80 cm³/min in humidity of 0–4 vol % H₂O, and it was monitored by multimeter (model 2701, Keithley Instruments Inc.). The sensor response (*S*) was defined as the ratio of electric resistance in synthetic air (*R*_a) and hydrogen gas (*R*_g).

RESULTS AND DISCUSSION

Characterization of Material. Figure 2 shows TEM images of SnO₂ and two typical Pd-loaded SnO₂ particles. Obviously Pd-loaded SnO₂ maintained the same morphology as neat SnO₂ particles. The average particle sizes of neat SnO₂ and both kinds of Pd-loaded SnO₂ were almost the same, about 15 nm. However, no Pd was directly observed by TEM due to its low amount. X-ray diffraction demonstrated that all the samples exhibited the same tetragonal phase (JCPDS: 41-1445). No phase corresponding to Pd or PdO was detected in the Pd-loaded SnO₂ powders due to extremely low Pd amount. It was not shown here for simplicity. Pd-loaded SnO₂ and neat SnO₂ have no obvious difference in the particle size, crystallite size, and specific surface area, meaning that the morphology of Pd-SnO₂ powder was independent of Pd and its loading method, as shown in Table 1. This is in agreement with a previous report that Pd has no influence to the morphology of SnO₂ by introducing it on the calcined SnO₂ surface.⁸ Thus, we can eliminate the influence of morphology on sensor response, and only focus on the effect of Pd size and its distribution state on the gas sensing properties.

Figure 3 shows Pd loading amount as a function of the precursor concentration for two kinds of Pd-loading methods. In

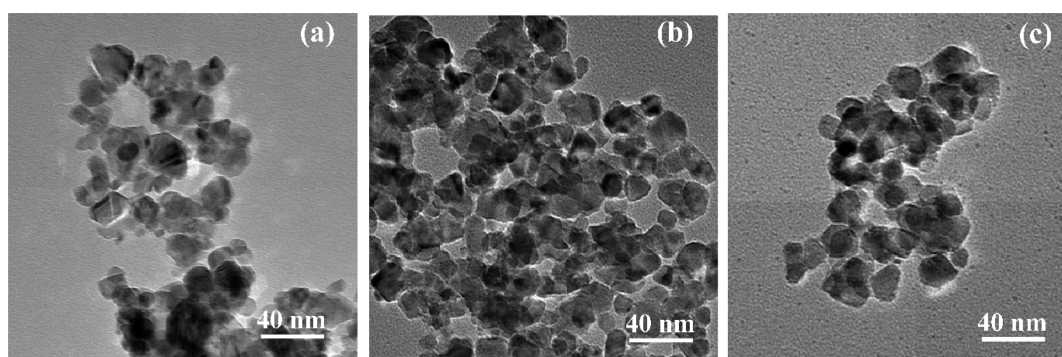


Figure 2. TEM images of SnO₂ (a), 0.7% PdNN-SnO₂ (b), and 0.5% PdN-SnO₂ (c).

Table 1. Particle Size, Crystallite Size, and Specific Surface Area for SnO₂ and Pd-Loaded SnO₂, as well as Pd Amount, Particle Size, Dispersion, and Surface Area of Pd for Pd-Loaded SnO₂

sample	particle size of SnO ₂ (nm) ^a	crystallite size of SnO ₂ (nm)	specific surface area (m ² /g)	Pd amount (mol %)	particle size of Pd (nm) ^b	dispersion of Pd (%) ^b	surface area of Pd (m ² /g) ^b
SnO ₂	14.8	11.7	27.1				
0.1% PdN-SnO ₂		11.9	28.4	0.09	3.5	32	0.10
0.3% PdN-SnO ₂		11.5	27.9	0.27	4.6	24	0.23
0.5% PdN-SnO ₂	15.1	11.6	29.9	0.47	5.3	21	0.31
0.7% PdN-SnO ₂		12.0	28.7	0.68	10.3	11	0.24
0.7% PdNN-SnO ₂	15.6	11.8	27.1	0.42	2.6	43	0.65

^aParticle size of SnO₂ was measured by TEM observation. ^bParticle size of Pd, dispersion of Pd, and surface area of Pd were measured by the CO pulse adsorption method. Dispersion of Pd was defined as the ratio of Pd atoms available for CO chemisorption to the total Pd atoms. Surface area of Pd means the surface area of Pd per 1 g of SnO₂ powder.

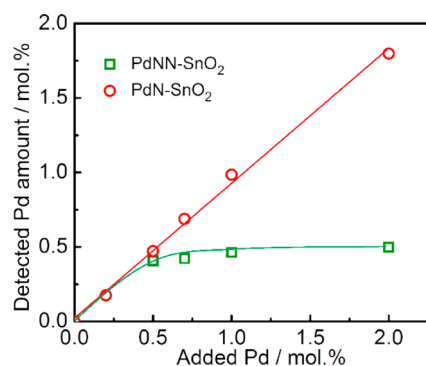


Figure 3. Pd loading amount as a function of the precursor concentration.

the case of PdNN-SnO₂, the Pd loading amount reached a saturation level when the precursor concentration increased to 0.7 mol %. It seems that the weak adhesion of Pd to the SnO₂ surface leads to Pd dispersing in solution. Thus, most of Pd was dispersed in solution when the Pd precursor concentration was above 0.7 mol %, and it was removed by the filtration process. On the other hand, in the case of PdN-SnO₂, Pd loading amount increased with increasing Pd added amount because Pd(NO₃)₂ solution directly mixed with SnO₂ and almost no Pd was lost in the preparation process. The actual Pd loading amount, particle size, dispersion and surface area of Pd on SnO₂ for Pd-loaded SnO₂ were compared in Table 1. The obtained total Pd amount on the SnO₂ surface was similar for 0.7% PdNN-SnO₂ and 0.5% PdN-SnO₂, although a different Pd amount was introduced in the material preparation process. Interestingly, it is found that Pd was loaded on the SnO₂ surface in a different distribution state for two kinds of Pd introduction methods. In the case of PdN-SnO₂, Pd particle size increased from 3.5 to 10.3 nm with increasing Pd

added amount. However, PdNN-SnO₂ gave smaller Pd (2.6 nm); even the Pd added amount increased to 0.7 mol %. With almost the same Pd loading amount, 0.7% PdNN-SnO₂ and 0.5% PdN-SnO₂ are characterized by smaller Pd particles with high dispersion and larger Pd particles with low dispersion, respectively. The effect of the Pd distribution state on the gas sensing properties was investigated in dry and humid atmospheres in the following section.

Oxygen Adsorption Behavior at Different Humidities.

Oxygen adsorption on the SnO₂ surface is a vital step for gas sensing. It is necessary to clarify the oxygen adsorption behavior in order to further understand the gas sensing mechanism. Therefore, the dependence of electric resistance on oxygen partial pressure in dry and humid atmospheres at 350 °C was studied in Figure 4. In dry atmosphere, the electric resistances of neat SnO₂ and Pd-loaded SnO₂ were linearly proportional to $P_{O_2}^{1/4}$ in the measured range (Figure 4b). Such a linear relationship agreed with the previous reports.^{2,16–18} Yamazoe et al. proposed a theoretical model and formulas about the relationship between electric resistance and oxygen partial pressure in volume depletion state of spherical SnO₂. According to the adsorbed oxygen species O⁻ and O²⁻ on the SnO₂ surface, the following two equations were proposed:

$$\frac{R}{R_0} = \frac{3}{a}(K_1 P_{O_2})^{1/2} + c \quad (O^- \text{ formation}) \quad (1)$$

$$\frac{R}{R_0} = \left\{ \frac{1}{4}c^2 + \frac{6N_D}{a}(K_2 P_{O_2})^{1/2} \right\}^{1/2} + c \quad (O^{2-} \text{ formation}) \quad (2)$$

Here R_0 is the electric resistance at flat-band condition, a grain radius, c a constant, N_D donor density, and K_1 and K_2 equilibrium

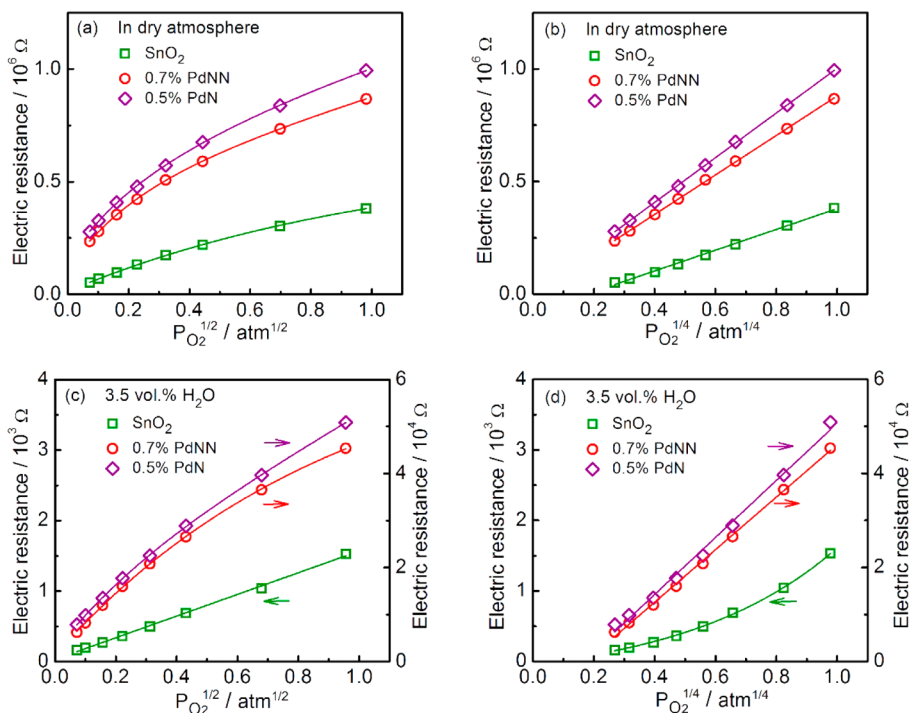


Figure 4. Dependence of the electric resistance on the $P_{O_2}^{1/2}$ and $P_{O_2}^{1/4}$ in dry and humid atmospheres at 350 °C: (a, b) dry; (c, d) 3.5 vol % H_2O .

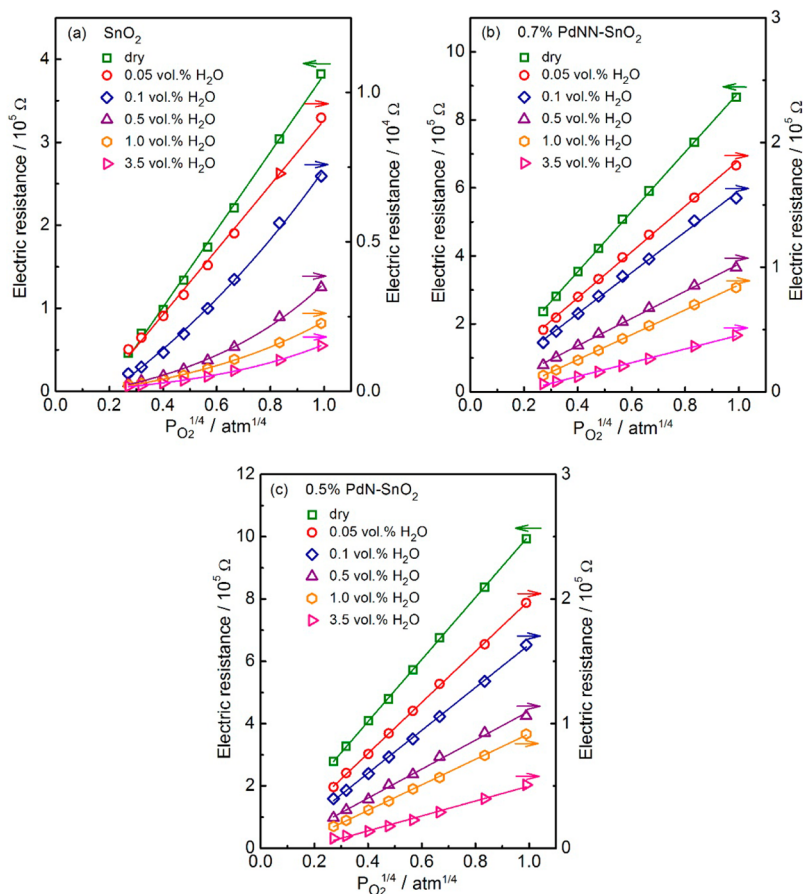


Figure 5. Dependence of the electric resistance on $P_{O_2}^{1/4}$ at different humidities at 350 °C: (a) SnO_2 , (b) 0.7% PdNN- SnO_2 , (c) 0.5% PdN- SnO_2 .

constants of adsorption. On the basis of the above equations, we can judge the oxygen species by measuring the electric resistance change with oxygen partial pressure. Therefore, it can be

concluded that the mainly adsorbed oxygen species was O^{2-} on SnO_2 and Pd- SnO_2 surfaces in dry atmosphere according to eq 2, due to the linear relationship of the electric resistance with $P_{O_2}^{1/4}$.

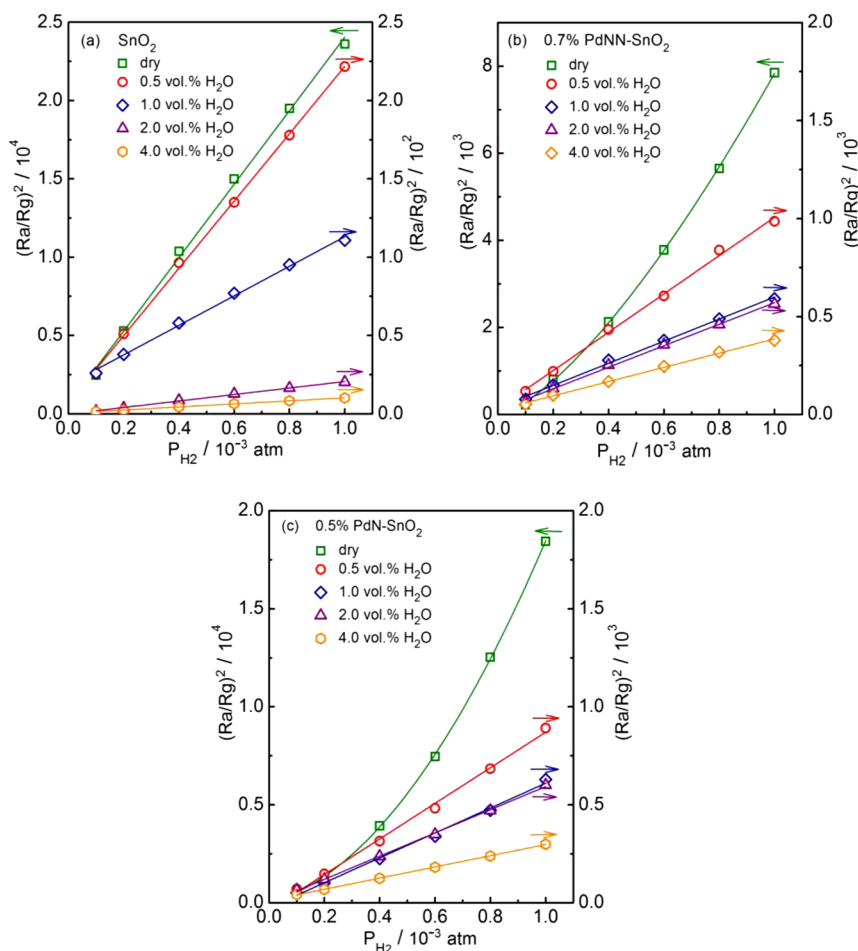


Figure 6. Dependence of $(R_a/R_g)^2$ on P_{H_2} at different humidities at 350 °C: (a) SnO_2 , (b) 0.7% PdNN-SnO₂, (c) 0.5% PdN-SnO₂.

At a humidity of 3.5 vol % H₂O (Figure 4c,d), the electric resistance was linearly proportional to $P_{O_2}^{1/2}$ for neat SnO_2 , meaning that the oxygen adsorption species was changed to O^- in wet atmosphere according to eq 1. The results were in agreement with the previous report for neat SnO_2 .¹⁸ Two kinds of Pd-loaded SnO_2 showed totally different oxygen adsorption behavior from neat SnO_2 in humid atmosphere, and a linear proportion of electric resistance to $P_{O_2}^{1/4}$ was observed in humid atmosphere. This means that the mainly adsorbed oxygen species undergo no change from dry to humid atmosphere, adsorbing as O^{2-} on the surface. The Pd distribution state had no difference in oxygen adsorption behavior at 350 °C. In addition, the electric resistance was greatly enhanced by loading Pd.

Figure 5 shows the dependence of electric resistance on $P_{O_2}^{1/4}$ at different humidities at 350 °C for SnO_2 and Pd-loaded SnO_2 . For neat SnO_2 (Figure 5a), a linear relationship of electric resistance with $P_{O_2}^{1/4}$ was observed in dry and low humidity (0.05 vol % H₂O), but this gradually disappeared with increasing humidity. It seems the amount of O^{2-} was reduced with increasing humidity, leaving O^- as the mainly adsorbed oxygen species on the SnO_2 surface. However, for 0.7% PdNN-SnO₂ and 0.5% PdN-SnO₂, the linearity of electric resistance with $P_{O_2}^{1/4}$ had no change from dry to humid atmosphere, although the resistance reduced with increasing water vapor concentration (Figure 5b,c). It seems the mainly adsorbed oxygen species O^{2-} on the Pd-SnO₂ surface was not influenced by water vapor except that the numbers of oxygen adsorption sites decreased. Because OH^- groups compete with oxygen species to adsorb on the SnO_2

surface, they disturb the O^{2-} adsorption. However, the disturbance of water vapor to O^{2-} was suppressed by loading Pd. Pd may provide new adsorption sites for O^{2-} to make it more favorable than the adsorption of water vapor. It turned out that the oxygen adsorption behavior was changed by loading Pd.¹⁶

Sensor Response to H₂ and CO at Different Humidities.

Figure 6 shows the square of sensor response as a function of hydrogen partial pressure at different humidities at 350 °C. The neat SnO_2 shows that the $(R_a/R_g)^2$ was linearly proportional to the P_{H_2} in both dry and humid atmospheres, as shown in Figure 6a. Such a linear relationship is in good agreement with the previously proposed theoretical equation in the volume depletion state of SnO_2 .²

$$\left(\frac{R_a}{R_g}\right)^2 = \left(\frac{3c}{aN_D}\right) \cdot P_{H_2} + 1 \quad (3)$$

Here R_a and R_g are the electrical resistances, respectively, in air and hydrogen gas, c a constant, a grain radius, N_D donor density, and P_{H_2} hydrogen partial pressure. In addition, the $(R_a/R_g)^2$ of neat SnO_2 was dramatically reduced about 100 times by introducing 0.5 vol % H₂O into the dry atmosphere. A nonlinear relationship of $(R_a/R_g)^2$ with P_{H_2} was observed for two kinds of Pd-loaded SnO_2 in dry atmosphere (Figure 6b,c). The $(R_a/R_g)^2$ was quickly increased in high hydrogen partial pressure, which seems to be due to the strong catalytic effect of PdO on H₂ oxidation on the SnO_2 surface. A similar phenomenon was also observed in the relationship of $(R_a/R_g)^2$ with P_{CO} for 0.7%

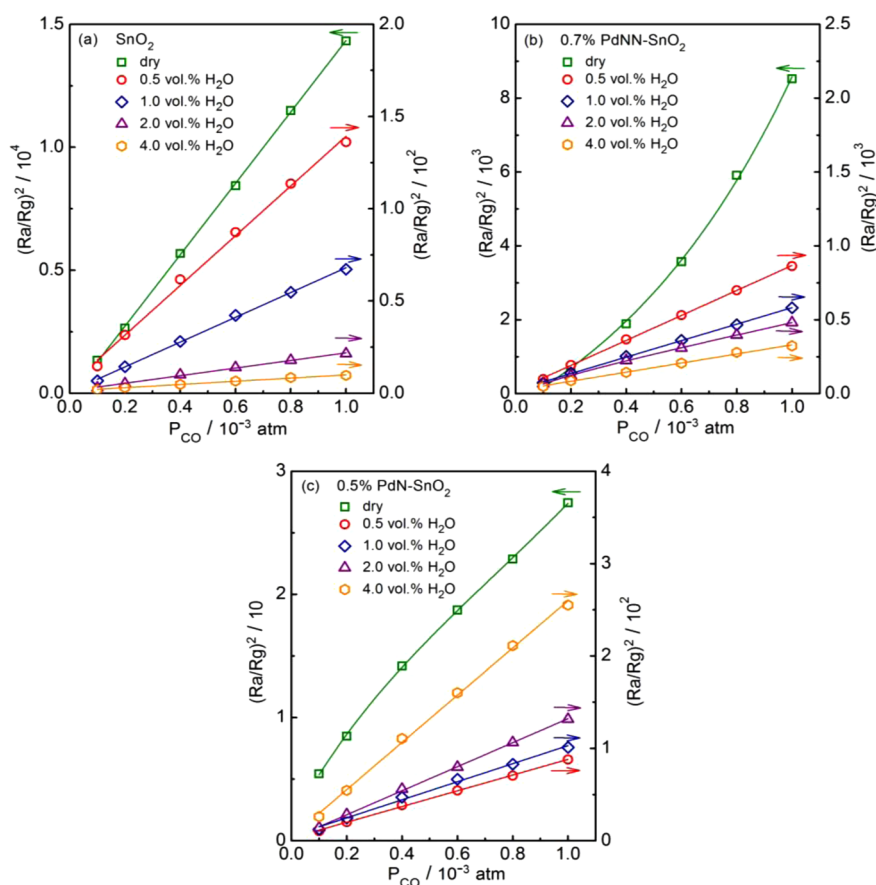


Figure 7. Dependence of $(R_a/R_g)^2$ on P_{CO} at different humidities at 350 °C: (a) SnO₂, (b) 0.7% PdNN-SnO₂, (c) 0.5% PdN-SnO₂.

PdNN-SnO₂ (Figure 7b). However, 0.5% PdN-SnO₂ showed a convex curve of $(R_a/R_g)^2$ with P_{CO} in dry atmosphere (Figure 7c). This may be due to the different catalytic ability of PdO to CO oxidation. It seems the 0.7% PdNN-SnO₂ with smaller Pd particle size has the stronger catalytic activity.

Figure 8 shows the electric resistance and sensor response to H₂ and CO as a function of water vapor concentration for neat SnO₂, 0.7% PdNN-SnO₂, and 0.5% PdN-SnO₂ at 300 and 350 °C. The electric resistance in air for all devices was reduced by introducing water vapor, which is especially remarkable for neat SnO₂, as shown in Figure 8a,a'. This means that the oxygen adsorption behavior was changed by loading Pd, as already mentioned. When comparing the enhancement of electric resistance by Pd loading between 0.7% PdNN-SnO₂ and 0.5% PdN-SnO₂, that of 0.5% PdN-SnO₂ was larger. This result shows that 0.5% PdN-SnO₂ forms a stronger P–N junction. As a result, the sensor response to H₂ at 300 °C for 0.5% PdN-SnO₂ was higher than that for 0.7% PdNN-SnO₂ (Figure 8b). At 350 °C, it was thought that H₂ gas was easily oxidized, so the sensor response of both elements became almost the same (Figure 8b'). However, the CO sensing behavior with humidity for 0.5% PdN-SnO₂ was different from that for 0.7% PdNN-SnO₂ at 300 °C, as shown in Figure 8c. In dry atmosphere, the sensor response of 0.5% PdN-SnO₂ was much lower than that for 0.7% PdNN-SnO₂, and the difference became wider by raising the operating temperature (Figure 8c'). The reason is that the electrical resistance was reduced less in CO; that is, PdO on the SnO₂ surface for 0.5% PdN-SnO₂ seems not easily to be reduced in dry atmosphere. Once introducing water vapor, the electric resistance quickly went down and the sensor response went

up. The reason why 0.5% PdN-SnO₂ showed such properties is not experimentally clear yet. However, if possible, the water-CO shift reaction may be one of the possible candidates to explain it. CO and H₂O react on the PdO surface and form CO₂ and H₂, resulting that 0.5% PdN-SnO₂ respond to H₂. Usually such a reaction occurs in the absence of oxygen, but it seems to be possible that the formed H₂ immediately reacts with PdO. To clarify such a reaction on 0.5% PdN-SnO₂, further investigations are necessary.

Analysis of Pd Size Effect. As mentioned above, the Pd size effect on the gas sensing properties of Pd-loaded SnO₂ was confirmed. To further investigate it, CO response at 350 °C for PdNN-SnO₂ and PdN-SnO₂ with different Pd amount is shown in Figure 9. All the PdNN-SnO₂ sensors showed the same CO sensing behavior with increasing humidity (Figure 9a). However, the CO response behavior of PdN-SnO₂ sensor greatly changed by Pd loading amount. The CO response behavior of 0.1% PdN-SnO₂ (Pd size: 3.5 nm in Table 1) was same as that of PdNN-SnO₂, but it was changed with increasing Pd loading amount (Pd size), as shown in Figure 9b. On the basis of these results, obviously smaller Pd particles showed stronger catalytic activity. Such difference in catalytic activity between 0.7% PdNN-SnO₂ and 0.5% PdN-SnO₂ was compared by TPR measurement. Figure 10 shows H₂O and CO₂ emission spectra of H₂-TPR and CO-TPR for neat SnO₂, 0.7% PdNN-SnO₂ and 0.5% PdN-SnO₂. In Figure 10a, H₂O emission spectra for 0.7% PdNN-SnO₂ and 0.5% PdN-SnO₂ were different from those for neat SnO₂. In the case of neat SnO₂, large peak was observed in the range of 300–400 °C. This peak seems to be due to O²⁻ and O⁻ adsorption on SnO₂ surface as reported previously.¹⁶ However, there was no

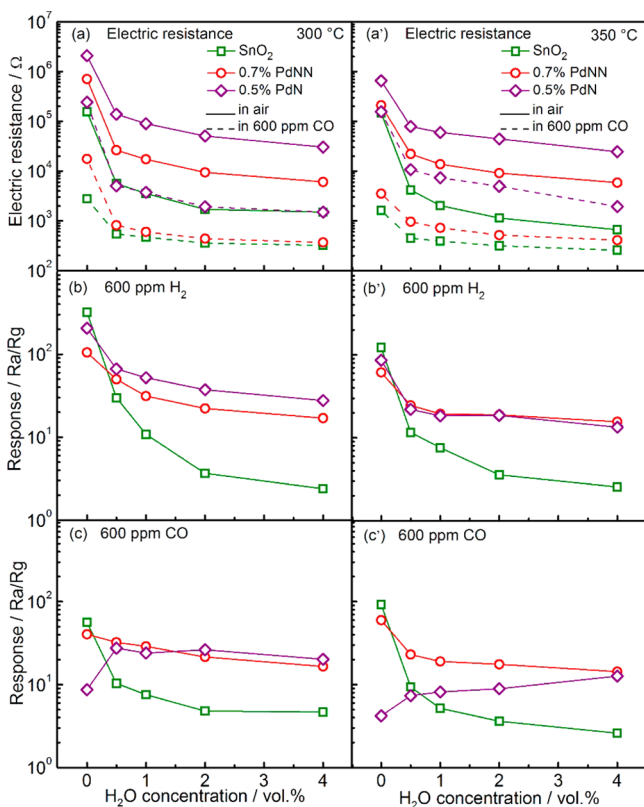


Figure 8. Gas sensing properties to reducing gas at different humidities at 300 (a–c) and 350 °C (a'–c'): (a, a') electric resistance in air and 600 ppm of CO; (b, b') response to 600 ppm of H₂; (c, c') response to 600 ppm of CO.

difference between 0.7% PdNN-SnO₂ and 0.5% PdN-SnO₂ except emission amount of H₂O. Both Pd-SnO₂ showed two large peaks at 180 and 250 °C. In the CO₂ emission spectra of CO-TPR (Figure 10b), a different point from H₂-TPR was that showed a peak at 300 °C. However, the most interesting point is that peaks of 0.7% PdNN-SnO₂ shifted a little to lower temperature as compared with that of 0.5% PdN-SnO₂. This means that 0.7% PdNN-SnO₂ is more catalytically active. Therefore, PdNN-SnO₂ showed high sensor response and stability under humid condition. The peak at high temperature may be considered by partially reduction of SnO₂ surface because SnO₂ surface was reduced catalytically by Pd under CO existence.¹⁹

The sensor response is closely related to the catalytic properties of the sensing layer. However, the Pd size and the dispersion are some of the most important factors affecting the activity. Many papers report the particle size effect of the noble metal catalyst involved in reducing gas (H₂, CO, and CH₄) oxidation.^{20–22} In such a case, the response of the gas sensor greatly depends on the Pd dispersion, since the catalytic activity relates to the dispersion.^{10,20,23} The influence of water vapor on the gas sensing properties is complicated and controversial. For the response to H₂, all the sensors showed a similar change in humid atmosphere, reducing sensor response with increasing humidity. This is similar to previous reports²⁴ and can be explained by the competing reaction with adsorbed oxygen species between H₂ and water vapor. In the case of CO, neat SnO₂ and 0.7% PdNN-SnO₂ showed a decreasing tendency in sensor response with increasing humidity, which was the same as the case of H₂ sensing. The CO response of 0.5% PdN-SnO₂ was even increased in humid atmosphere. We considered that the different Pd/PdO distribution state leads to the different sensitization effect on CO oxidation in humid atmosphere. However, the enhancing effect of water vapor on CO response for 0.5% PdN-SnO₂ is under consideration, and the detailed reaction mechanism needs to be further clarified. Regardless of sensing to H₂ or CO, it is doubtless that smaller Pd particles on SnO₂ suppress the water vapor poisoning effect on sensor response.

CONCLUSIONS

The Pd size effect on the gas sensor performance at different humidities was analyzed based on Pd-loaded SnO₂ with smaller and larger Pd particle sizes. The adsorbed oxygen species was the same for two kinds of Pd-loaded SnO₂, that is, O²⁻ in both dry and humid atmospheres. An interfering effect of water vapor on H₂ response was observed for both Pd-loaded SnO₂ sensors. However, in the case of CO response, Pd-SnO₂ with smaller Pd particles was reduced by introducing water vapor but kept high stability with varying humidity, while Pd-SnO₂ with large Pd particles showed increased CO response in the presence of water vapor and it was increased with the rising humidity. This different behavior toward CO sensing was explained by the different catalytic activities of Pd particles when they were in different distribution states. The Pd size and amount, which one is the key factor to reduce the water vapor effect on the gas sensing performance, or how to load high amounts of Pd particles with

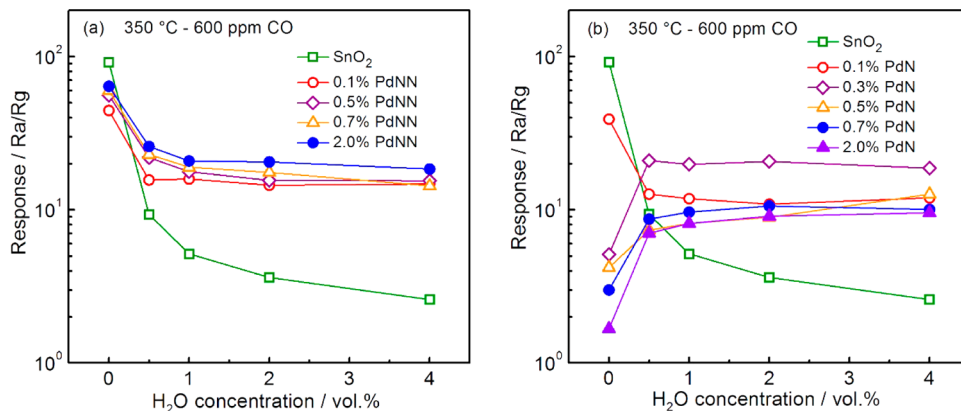


Figure 9. Sensor response to 600 ppm of CO for PdNN-SnO₂ (a) and PdN-SnO₂ (b) with different Pd amounts at different humidities at 350 °C.

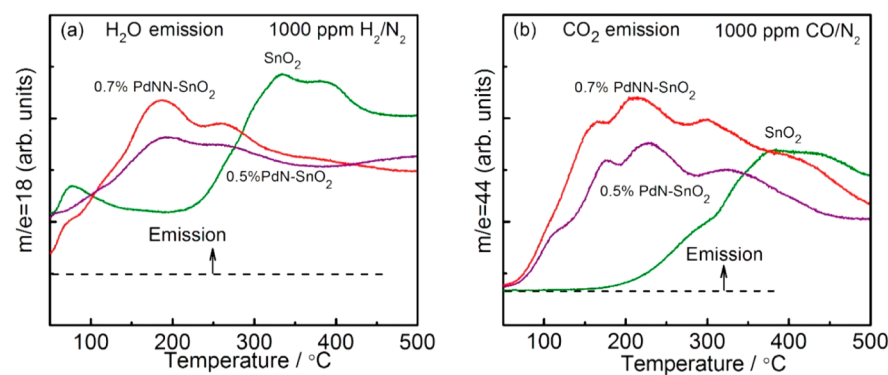


Figure 10. H₂O and CO₂ emission spectra of H₂-TPR (a) and CO-TPR (b) for neat SnO₂ and Pd-loaded SnO₂.

smaller size (<3.5 nm) on a SnO₂ surface, are meaningful research areas to pursue in the future.

AUTHOR INFORMATION

Corresponding Author

*E-mail: shimanoe.kengo.695@m.kyushu-u.ac.jp.

Notes

The authors declare no competing financial interest.

REFERENCES

- (1) Barsan, N.; Weimar, U. Understanding the Fundamental Principles of Metal Oxide Based Gas Sensors; the Example of CO Sensing with SnO₂ Sensors in the Presence of Humidity. *J. Phys.: Condens. Matter* **2003**, *15*, 813–839.
- (2) Yamazoe, N.; Suematsu, K.; Shimanoe, K. Extension of Receptor Function Theory to Include Two Types of Adsorbed Oxygen for Oxide Semiconductor Gas Sensors. *Sens. Actuators, B* **2012**, *163*, 128–135.
- (3) Großmann, K.; Wicker, S. E.; Weimar, U.; Barsan, N. Impact of Pt Additives on the Surface Reactions between SnO₂, Water Vapour, CO and H₂; an Operando Investigation. *Phys. Chem. Chem. Phys.* **2013**, *15*, 19151–19158.
- (4) Koziej, D.; Barsan, N.; Shimanoe, K.; Yamazoe, N.; Szuber, J.; Weimar, U. Spectroscopic Insights into CO Sensing of Undoped and Palladium Doped Tin Dioxide Sensors Derived from Hydrothermally Treated Tin Oxide Sol. *Sens. Actuators, B* **2006**, *118*, 98–104.
- (5) Safonova, O.; Neisius, T.; Ryzhikov, A.; Chenevier, B.; Gaskov, A.; Labeau, M. Characterization of the H₂ Sensing Mechanism of Pd-Promoted SnO₂ by XAS in Operando Conditions. *Chem. Commun.* **2005**, *41*, S202–S204.
- (6) Matsushima, S.; Maekawa, T.; Tamaki, J.; Miura, N.; Yamazoe, N. New Methods for Supporting Palladium on a Tin Oxide Gas Sensor. *Sens. Actuators, B* **1992**, *9*, 71–78.
- (7) Cabot, A.; Dieguez, A.; Romano-Rodriguez, A.; Morante, J. R.; Barsan, N. Influence of the Catalytic Introduction Procedure on the Nano-SnO₂ Gas Sensor Performances Where and How Stay the Catalytic Atoms? *Sens. Actuators, B* **2001**, *79*, 98–106.
- (8) Dieguez, A.; Vila, A.; Cabot, A.; Romano-Rodriguez, A.; Morante, J. R.; Kappler, Barsan, N.; Weimar, U.; Gopel, W. Influence on the Gas Sensor Performances of the Metal Chemical States Introduced by Impregnation of Calcinated SnO₂ sol–gel nanocrystals. *Sens. Actuators, B* **2000**, *68*, 94–99.
- (9) Cabot, A.; Arbiol, J.; Morante, J. R.; Weimar, U.; Barsan, N.; Gopel, W. Analysis of the Noble Metal Catalytic Additives Introduced by Impregnation of as Obtained SnO₂ Sol-Gel Nanocrystals for Gas Sensors. *Sens. Actuators, B* **2000**, *70*, 87–100.
- (10) Cabot, A.; Arbiol, J.; Morante, J. R. Analysis of the Catalytic Activity and Electrical Characteristics of Different Modified SnO₂ Layers for Gas Sensors. *Sens. Actuators, B* **2002**, *84*, 12–20.
- (11) Lim, C. B.; Oh, S. Microstructure Evolution and Gas Sensitivities of Pd-Doped SnO₂-Based Sensor Prepared by Three Different Catalyst-Addition Processes. *Sens. Actuators, B* **1996**, *30*, 223–231.
- (12) Schmid, W.; Barsan, N.; Weimar, U. Sensing of Hydrocarbons and CO in Low Oxygen Conditions with Tin Dioxide Sensors: Possible Conversion Paths. *Sens. Actuators, B* **2004**, *103*, 362–368.
- (13) Kimura, K.; Einaga, H.; Teraoka, Y. Preparation of Highly Dispersed Platinum Catalysts on Various Oxides by Using Polymer-Protected Nanoparticle. *Catal. Today* **2011**, *164*, 88–91.
- (14) Einaga, H.; Urahama, N.; Tou, A.; Teraoka, Y. CO Oxidation over TiO₂-Supported Pt–Fe Catalysts Prepared by Coimpregnation Methods. *Catal. Lett.* **2014**, *144*, 1653–1660.
- (15) Einaga, H.; Mochiduki, K.; Teraoka, Y. Photocatalytic Oxidation Processes for Toluene Oxidation over TiO₂ Catalysts. *Catalysts* **2013**, *3*, 219–231.
- (16) Ma, N.; Suematsu, K.; Yuasa, M.; Kida, T.; Shimanoe, K. Effect of Water Vapor on Pd-Loaded SnO₂ Nanoparticles Gas Sensor. *ACS Appl. Mater. Interfaces* **2015**, *7*, 5863–5869.
- (17) Suematsu, K.; Yuasa, M.; Kida, T.; Yamazoe, N.; Shimanoe, K. Determination of Oxygen Adsorption Species on SnO₂: Exact Analysis of Gas Sensing Properties Using a Sample Gas Pretreatment System. *J. Electrochem. Soc.* **2014**, *161*, 123–128.
- (18) Yamazoe, N.; Suematsu, K.; Shimanoe, K. Gas Reception and Signal Transduction of Neat Tin Oxide Semiconductor Sensor for Response to Oxygen. *Thin Solid Films* **2013**, *548*, 695–702.
- (19) Shimanoe, K.; Arisuda, S.; Oto, K.; Yamazoe, N. Influence of Reduction Treatment on CO Sensing Properties of SnO₂-Based Gas Sensor. *Electrochemistry* **2006**, *74*, 183–185.
- (20) Kocemba, I.; Rynkowski, J. The Influence of Catalytic Activity on the Response of Pt/SnO₂ Gas Sensors to Carbon Monoxide and Hydrogen. *Sens. Actuators, B* **2011**, *155*, 659–666.
- (21) Chen, X. Y.; Cheng, Y. S.; Seo, C. Y.; Schwank, J. W.; McCabe, R. W. Aging, Re-dispersion, and Catalytic Oxidation Characteristics of Model Pd/Al₂O₃ Automotive Three-way Catalysts. *Appl. Catal., B* **2015**, *163*, 499–509.
- (22) Haruta, M.; Yamada, N.; Kobayashi, T.; Iijima, S. Gold Catalysts Prepared of Coprecipitation for Low-Temperature Oxidation of Hydrogen and Carbon Monoxide. *J. Catal.* **1989**, *115*, 301–309.
- (23) Li, G. J.; Zhang, X. H.; Kawi, S. Relationships between Sensitivity, Catalytic Activity, and Surface Areas of SnO₂ Gas Sensors. *Sens. Actuators, B* **1999**, *60*, 64–70.
- (24) Pavelko, R.; Daly, H.; Hardacre, C.; Vasilieva, A.; Llobeta, E. Interaction of Water, Hydrogen and Their Mixtures with SnO₂ Based Materials: the Role of Surface Hydroxyl Groups in Detection Mechanisms. *Phys. Chem. Chem. Phys.* **2010**, *12*, 2639–2647.